

Design of Mechanical and Electrical Control System of Mixed Liquid Gas Pressure Energy Storage Based on Maximum Power Point Tracking

Jia Zhang

Fundamental Experiment Training Center, Tianjin Sino-German University of Applied Sciences, Tianjin 300350, China

Received July 18 2020

Accepted March 18 2021

Abstract

In order to solve the problem that the accuracy of the controller of the traditional mechanical control system is not high and the efficiency of the control system is too low, a mechanical control system based on maximum power point tracking is designed. Through the controller platform, the embedded microprocessor with arm architecture is used to design the basic peripheral circuit, and to improve the control accuracy of the controller, and to complete the hardware design of the system. According to the characteristics of the compression efficiency of the liquid pump, the energy storage device is modeled, the maximum power point tracking algorithm is used to control the speed of the motor, and the software design of the system is completed. Regarding the hardware and software design of the system, the mechanical and electrical control system design of the mixed liquid gas pressure energy storage device is realized. The experimental results show that the design system is basically consistent with the standard control value, the system efficiency is the largest, and the mechanical and electrical control accuracy of the mixed oil and gas energy storage is improved, and the active power can reach a stable state.

© 2021 Jordan Journal of Mechanical and Industrial Engineering. All rights reserved

Keywords: Maximum power point tracking; Mixed liquid gas pressure energy storage machine; Control system; Efficiency value;

1. Introduction

With the wide application of new energy generation, energy storage technology has been developed rapidly. Because of the location of Micro Capacity compressed air energy storage system, and its cost which is relatively low, it has been widely used. Micro capacity compressed air energy storage has become a new technology of renewable energy generation and energy storage system. In the air energy storage technology, in order to improve the efficiency, we can start from the thermodynamic principle. At the same time, the energy conversion efficiency in electromechanical conversion has a great influence on the energy storage system. In the traditional air compression energy storage system, asynchronous motor is mainly used, and the traditional motor control mode is used to compress the air to obtain energy. But the disadvantage of this technology is its low efficiency [1]. The system is a hybrid energy storage system, which includes liquid gas hybrid pressure energy storage system, high energy density air compression energy storage device and high-power density super capacitor energy storage device. Because the conversion of mechanical and electrical energy has a great influence on the efficiency of the system, in the system of liquid gas mixed energy storage and compression, the

research on the compressed air energy storage system has made some progress in recent years.

A combined automatic generation control system of thermal power unit and energy storage system is proposed and designed in document [2]. The basic principle, typical scheme, control process and practical engineering effect of the technology are introduced. The influence of the connection mode of the energy storage system on the electrical system of thermal power unit and the selection of the storage battery are discussed. The investment and income of the technology in engineering application are analyzed. The analysis results show that the combination of AGC frequency modulation technology with thermal power unit and energy storage system has remarkable effect and good economic benefit. The access of energy storage system has no influence on the control system and electrical system of thermal power unit. As the battery of energy storage system, lithium iron phosphate battery has many advantages, which provides reference for the practical engineering application of AGC frequency modulation technology combined with thermal power unit and energy storage system. However, the accuracy of the system is low, which leads to the instability of the active power. A multi-port power generation control system based on energy storage is proposed and designed in document [3]. According to the system requirements, the structure and function of each part are designed. The energy management scheme and configuration strategy of the energy storage unit

* Corresponding author e-mail: zhangjiantianjin@126.com.

are analyzed. The fuel cell adopts one-way dc/dc converter, voltage and current double closed-loop control. Through the energy storage unit and bidirectional dc/dc converter, the load and super capacitor energy storage unit are provided with energy when the dynamic change is in progress. The sliding mode control and the segment PI control strategy are adopted to realize the fast transfer control of energy and improve the output stability of the system. The simulation model of the system is established to verify the effectiveness of the multi-port power system control strategy. But the efficiency of the liquid pump in this system is low, and there are some hidden dangers.

In view of the problems in the above system, a new type of mechanical and electrical control system for liquid gas mixed energy storage is designed by using the maximum power point tracking strategy. The invention combines the high energy density air compression energy storage device and the super capacitor energy storage device with high power density into a hybrid energy storage system. The hybrid liquid compression energy storage system is controlled by permanent magnet synchronous motor. For the system, the maximum efficiency point tracking algorithm is used to control the motor of the system, so that the motor load liquid pump works at the maximum efficiency point, thus improving the mechanical and electrical conversion efficiency of the system. The experimental results show that the method can be used for reference, improve the conversion efficiency of electromechanical energy, and provide the basis for the construction and work of hybrid energy storage system.

2. Hardware design of mechanical and electrical control system of mixed liquid gas pressure energy storage

2.1. Controller platform

The controller platform adopts ARM embedded microprocessor and embedded controller of $\mu C / OS - II$ real-time operating system in series. The hardware platform design of the controller is shown in Figure 1.

Figure 1 shows the structure, the CPU of the controller adopts Samsung's 32-bit RISC microprocessor S3C44BOX based on ARM7TDMI core, with the main frequency of 66 MHz. The chip integrates external memory controller, LCD controller, 4 DMA controllers and 2 darts, IIC and IIS bus controller, A / D, I / O and other interfaces, embedded controller system resources based on S3 c44box include: 8 MB SDRAM as system memory, 4MB flash as electronic disk, standard RS-232 serial communication interface. The embedded controller uses LCD and keyboard as human-computer interface, which has powerful human-computer interaction function [4].

In order to reduce the cost of the whole system, through 16 / 32-bit RISC processor S3C44BOX by using its own on-chip peripherals, a LMD18200 driver chip is connected outside the processor. The H-bridge and its control logic circuit composed of four DMOS are included in an 11 pin t-220 package. The rated current is 3 A, the peak current is 6 A, the voltage power is 55 V, and the on resistance of the power transistor is 0.3 Ω , TTL and CMOS compatible control signal input, including bridge arm single side through circuit; chip overheat alarm output and automatic shutdown. Settings LMD18200 Logical Menu Table 1.

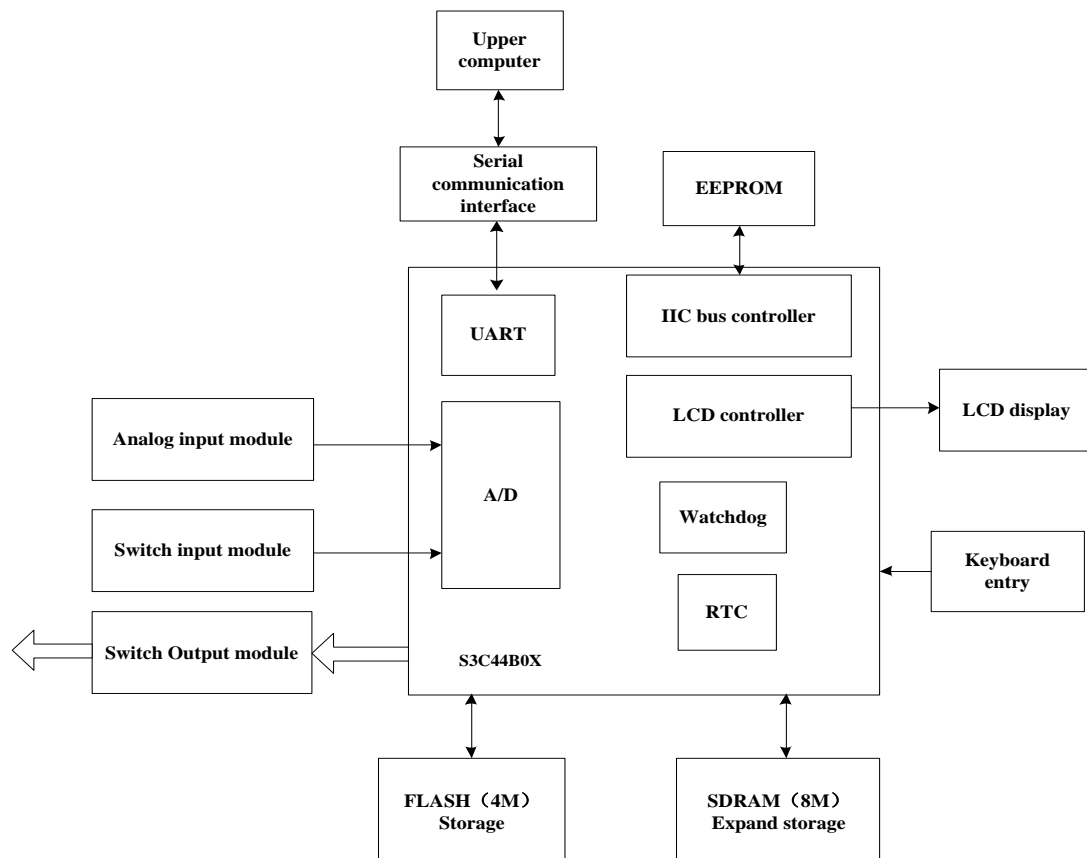


Figure 1. Hardware structure of controller

Table 1. LMD18200 logic menu

PWM	Turn	Enable	Actual output drive current	Motor working state
H	H	L	Outflow 1, inflow 2	Forward rotation
H	L	L	Inflow 1, outflow 2	Reversal
L	/	L	Outflow 1, outflow 2	Stop it
H	H	H	Outflow 1, outflow 2	Stop it
H	L	H	Inflow 1, inflow 2	Stop it
L	X	H	NONE	

Driven by the functions in Table 1, since the control signal of the motor is directly generated by the DSP, and the drive circuit of the DC motor is directly connected with a voltage of up to 26.2 V, if there is a problem in the circuit, the current will flow directly into the DSP, causing damage to the DSP and its peripheral circuits, so all the control signals and feedback signals must be isolated by the photoelectric isolation device to make the motor drive electricity. The circuit is completely separated from the DSP [5]. Even if there is a problem in the circuit, it will not cause great damage to the whole system. At the same time, the frequency of PWM signal in the control is relatively high for the photoelectric isolation device, and the common photoelectric isolation device such as 6N137 cannot be used. When the rectangular wave of PWM signal is input from the photoelectric isolation device, when the frequency is high, only trapezoidal wave can be obtained at the output end of the photoelectric isolation device, which cannot achieve accurate PWM control. Therefore, 6N137 high-speed optocoupler isolator is selected in this paper, which can fully adapt to high signal frequency. A schematic diagram of the connection to the DSP is shown in Figure 2.

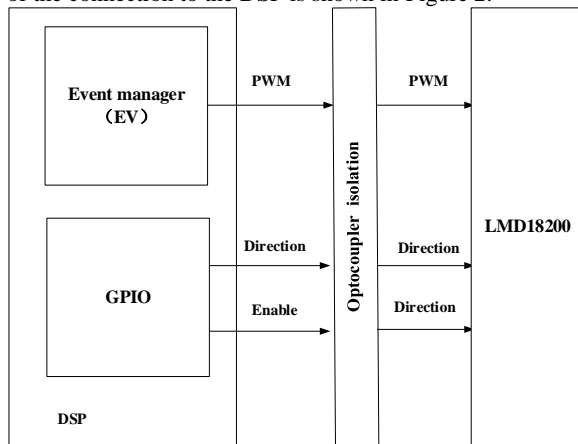


Figure 2. Connection diagram

As shown in Figure 2, the PWM pulse signal is generated by the F2812 event manager, while the direction signal and enable signal are programmed and controlled by the F2812 general input output (GPIO) bus. After the controller is

designed, the peripheral circuit is designed and the hardware part of the system is designed [6].

2.2. Basic peripheral circuit

When designing the basic peripheral circuit, first design the clock circuit. Because of the particularity of the control system, in this system, the S3C44BOX processor chip uses the passive crystal oscillator, and the connection method of crystal oscillator is shown in Figure 3.

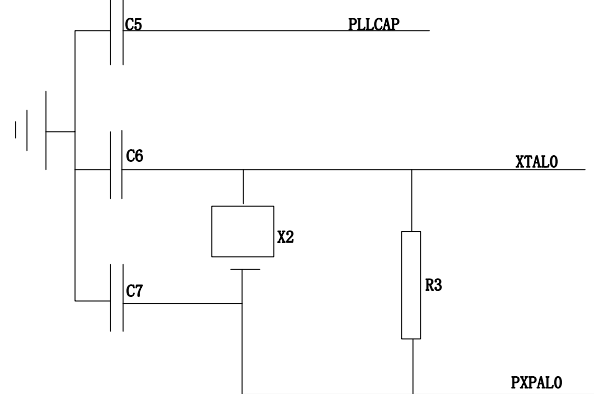


Figure 3. Clock circuit

The clock circuit connection diagram shown in Figure 3, according to the highest working frequency of S3C44BOX and the working mode of PLL circuit, 10 MHz passive crystal oscillator is selected. After 10 MHz crystal oscillator frequency is doubled by PLL circuit in S3C44BOX, the maximum can reach 66 MHz. The on-chip PLL circuit has the function of frequency amplification and signal purification. Therefore, the system can obtain a higher working frequency with a lower external clock signal to reduce the high-frequency noise caused by the high-speed switch clock [7].

The reset circuit mainly completes the power on reset of the system and the key reset function of the user when the system is running, and adopts a simple RC reset circuit. The designed reset circuit is shown in Figure 4.

From the reset circuit shown in Figure 4, when the system is powered on, charge the capacitor C1 through the resistance R1. When the voltage at both ends of C1 does not reach the threshold voltage of high level, the output of reset terminal is low level, and the system is in the reset state; when the voltage at both ends of C1 reaches the threshold voltage of high level, the output of reset terminal is high level, and the system enters the normal working state. When the user presses the button S1, the charge at both ends of C1 is discharged, the output of reset end is low level, the system enters the reset state, and then repeats the above charging process, the system enters the normal working state. Based on the above operations, the hardware design of the mechanical and electrical control system of mixed liquid gas pressure storage is completed, and the software part of the control system is designed according to the properties of mixed liquid gas pressure storage [8].

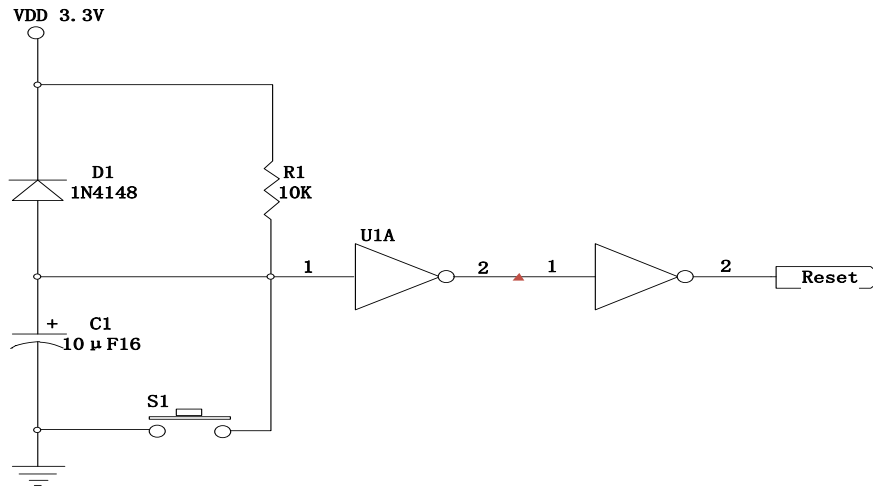


Figure 4. Reset circuit

3. Software design of mechanical and electrical control system of mixed liquid gas pressure energy storage

3.1. Characteristics of liquid pump

In the process of energy storage, the motor first converts energy from electrical energy to mechanical energy, and then the liquid pump, driven by mechanical energy, provides energy for the liquid in the liquid tank to be delivered to the gas tank. The liquid delivered to the gas tank by medium pressure, just like the liquid piston, compresses the gas in the gas tank, and then reserves the energy in this process. In the process of energy release, the high-pressure gas in the gas tank will send the liquid in the gas tank back to the liquid tank, at the same time, it also provides energy for the rotation of the hydraulic motor. The rotation of the motor drives the rotation of the motor, thus generating electric energy. The mechanical and electrical conversion link of the mixed liquid gas compression energy reserve system is mainly composed of the liquid pump and the motor. The liquid pump is the load of the motor, and the control of the motor will determine the working state of the liquid pump. Therefore, it is necessary to study the working characteristics of the liquid pump and optimize the control strategy of the motor based on this. The motor converts electrical energy into mechanical energy and outputs torque T_{sm} to the hydraulic pump. The rotational speed N of the motor can be calculated as follows:

$$N = \frac{1}{J} \int (T_{sm} - T_{hm}) dt \quad (1)$$

In the above formula, T_{hm} is the load torque of the liquid pump as the motor load, T_{sm} is the motor control torque, J is the inertia coefficient of the shaft, and the friction loss of the shaft is ignored. The liquid flow from the liquid tank to the liquid pump Q is:

$$Q = DN \quad (2)$$

where D is the displacement of the liquid pump, according to the standard gas equation:

$$\rho V = nRT \quad (3)$$

Among them, ρ , V , n , R and T are respectively expressed as the pressure, volume, quantity, temperature and constant of ideal gas. The product of pressure and

volume before and after gas compression is constant in the isothermal process, so we can get:

$$\rho_{am} V_s = \rho \left(V_s - \int_0^t Q dt \right) \quad (4)$$

where ρ_{am} is the standard atmospheric pressure and V_s is the volume of the air tank. According to the above formula, the pressure ρ of compressed gas can be calculated, and the torque expression of liquid pump can be calculated as follows:

$$\begin{cases} T_{hm} = \frac{\Delta P D}{2\pi} \\ \Delta P = P - \rho_{am} \end{cases} \quad (5)$$

According to the above formula (4) and formula (5), the efficiency of liquid pump is equal to the product of volume efficiency η_v and mechanical efficiency η_m , that is:

$$\eta_{pump} = \eta_v \times \eta_m \quad (6)$$

In the above formula, volume efficiency and mechanical efficiency have the following quantitative relationship:

$$\begin{cases} \eta_v = \frac{Q_{out}}{DN} \\ \eta_m = \frac{D\Delta p}{T_{sm} 2\pi} \end{cases} \quad (7)$$

where Q_{out} is the flow of liquid from the liquid pump. During the whole compression process, set the work efficiency of compressed gas as η_y , the motor efficiency as η_d , and the converter efficiency as η_{bv} . the total efficiency of the whole compression and energy storage process can be expressed as follows:

$$\eta_w = \eta_{bv} \frac{\eta_d}{\eta_y} \quad (8)$$

It can be seen from the above formula that according to the principle of thermodynamics, multiple compression and reduction of compression ratio can improve the work efficiency of compressed gas. The efficiency of permanent magnet synchronous motor is higher and less affected by load. Assuming that the motor efficiency and converter efficiency are fixed, the efficiency of liquid pump can be improved, which can effectively improve the total efficiency of the system [9].

According to the data provided by the liquid pump manufacturer, the compression efficiency characteristics of the liquid pump are shown in Figure 5.

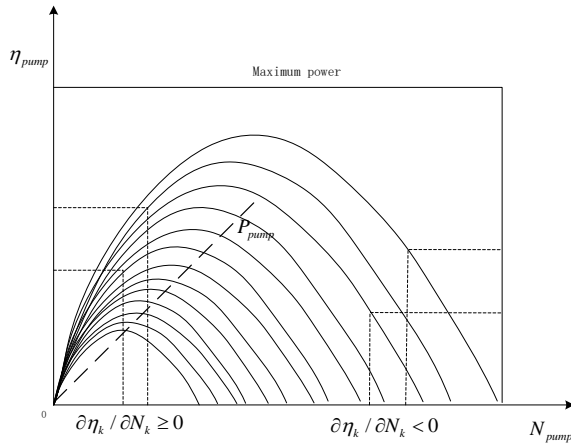


Figure 5. Working efficiency characteristics of liquid pump

As can be seen from Figure 5 that the sampling speed has the following quantitative relationship with the efficiency of the liquid pump:

$$\frac{\partial \eta_k}{\partial N_k} = \frac{\eta_k - \eta_{k-1}}{N_k - N_{k-1}} \quad (9)$$

where, N_k and η_k represent the rotational speed of k-sampling and the corresponding efficiency calculation value respectively. The rotational speed and pressure of the liquid pump determine the working efficiency of the liquid pump [10]. Therefore, in order to make the liquid pump work with higher efficiency, we should consider the pressure change and control the motor speed, so that the liquid pump works at the most reasonable speed [11].

3.2. Motor speed control based on maximum power point tracking

The liquid pump realizes the conversion from the kinetic energy of liquid to the mechanical energy of rotating shaft, which is represented by the mechanical conversion module. Combined with the above analysis of the working characteristics of the liquid pump, the energy storage device is modeled by using the characteristics of the input quantity as the speed and pressure difference, and the output quantity as the flow and the load torque of the motor. Based on the gas state equation, the calculation can be obtained:

$$\left(V_{air} - \int_0^t Q dt \right) p_a = p_{am} V_{air} \quad (10)$$

where V_{air} is the volume of the air tank. Since the inverter is connected with three-phase symmetrical load, only two variables need to be considered in modeling (the third variable can represent the three-phase voltage of the stator with the first two variables linearly). The three-phase voltage of the stator in the three-phase static coordinate system can be expressed as:

$$U = \frac{1}{3} \begin{bmatrix} 2 & -1 \\ -1 & 2 \\ -1 & -1 \end{bmatrix} U_{inv} \quad (11)$$

The stator voltage in the two-phase rotating coordinate system is calculated by the above formula. The calculation formula is as follows:

$$\begin{bmatrix} x_{sd} \\ x_{sq} \end{bmatrix} = \sqrt{\frac{2}{3}} \begin{bmatrix} \cos \theta & \cos(\theta - \frac{2\pi}{3}) & \cos(\theta + \frac{2\pi}{3}) \\ -\sin \theta & -\sin(\theta - \frac{2\pi}{3}) & -\sin(\theta + \frac{2\pi}{3}) \end{bmatrix} \begin{bmatrix} x_{s1} \\ x_{s2} \\ x_{s3} \end{bmatrix} \quad (12)$$

In the above formula, θ represents the angle difference between the rotor and the stator position, which can be obtained by rotating speed. The calculation formula is $\frac{d\theta}{dt} = N_p \omega$, N_p represents the pole pairs of the motor, and ω represents the shaft angular speed of the hydraulic pump. In this model, the motor consists of an energy accumulation module and an electromechanical conversion module. The motor current in the energy accumulation module can be obtained from the stator voltage and the motor electromotive force e :

$$L_s \frac{di}{dt} = (U - e) - ri_{line} \quad (13)$$

where, L_s and r are the stator inductance and winding resistance of the motor respectively. When the output voltage value is a specific value, the output power reaches the maximum value. Then the power consumed on the load internal resistance R_0 is:

$$P_{R_0} = I^2 R_0 = \left(\frac{V_p}{R_r + R_0} \right)^2 R_0 \quad (14)$$

where V_p is a constant. When the output power of the inverter is set as P_{R_0} , it can be seen that there is only one maximum point, that is, the maximum power point, and the derivation of load internal resistance R_0 can be obtained:

$$\frac{dP_{R_0}}{dR_0} = \frac{(R_r - R_0)V_p^2}{(R_r + R_0)^3} \quad (15)$$

where V is the voltage source voltage and R_r is the internal resistance of the voltage source. According to the two ends of the above formula, and then the derivation of R_0 , we can get:

$$\frac{d^2 P_{R_0}}{dR_0^2} = \frac{2R_0 - 4R_r}{(R_r + R_0)^4} \quad (16)$$

Let $\frac{dP_{R_0}}{dR_0} = 0$, get $R_r = R_0$, substitute it into formula (16), get $\frac{d^2 P_{R_0}}{dR_0^2} = \frac{-2R_r}{(R_r + R_0)^2} < 0$. Therefore, when the

output power P_{R_0} is the maximum value, $R_r = R_0$. That is, when the internal resistance of the load and the internal resistance of the power supply are equal, the output power reaches the maximum value. For a linear circuit with constant internal resistance, the external resistance of the load can be adjusted to make its resistance equal to the internal resistance value, so as to obtain the maximum power point, that is, the optimal working point [12].

The torque of motor and liquid pump is added to the shaft to generate the motor speed. The maximum power point obtained from the above formula is used to control the motor speed. The expression is:

$$J \frac{d\omega}{dt} = T_{sm} - T_{hm} - f\omega \quad (17)$$

where f is the coefficient of friction.

3.3. Implementation control

Based on the maximum power point control and maximum efficiency point control algorithm, the inversion control module of the control system is realized by programming and PI control. The calculation formula is as follows:

$$T_{sm_ref} = \text{Cont}[w_{ref} - w_{mes}] + T_{sm} \quad (18)$$

In the above formula, $\text{Cont}[w_{ref} - w_{mes}]$ represents the controller of variable, which is generally implemented by PI controller. T_{sm_ref} is the reference value of motor torque. The motor module is inverted, and the motor winding module is used as the energy accumulation module. The controller is used to realize the inversion operation, and the reference value and measurement value of the stator current are obtained [13-15]. Under the measured value, the park transform is inverted as follows, and the voltage reference value of the inverter is calculated. Using the voltage reference value, the reference value of the regulating amount is calculated, and the calculation formula is as follows:

$$m_{ref} = \frac{u_{ref}}{u_{cap}} \quad (19)$$

where, u_{rect_ref} is the reference value of inverter voltage

and u_{cap} is the measured value of inverter voltage. Starting from the calculated maximum reference value of the inverter, the tracking control flow of the maximum efficiency point of the energy storage system is shown in Figure 6.

Process according to the process shown in Figure 6, in the initial stage, the reference speed is given by using the quadratic interpolation method to make the liquid pump start quickly; after the start-up, the working point of the liquid pump is judged to be on the left or right side of the maximum efficiency point by using the working efficiency characteristic diagram of the liquid pump, so as to correct the speed and complete the tracking control of the maximum efficiency point of the liquid pump; the maximum power point tracking is calculated by using the power of the liquid pump to get the control strategy, when the motor power is less than the design power of the system, gives a higher reference speed, so that the system power increases rapidly, so as to quickly store energy; when the motor power reaches the design power of the system, calculate the reference speed of the system at the maximum power, so as to control the system at the maximum power point. Finally, the software design of the control system is completed.

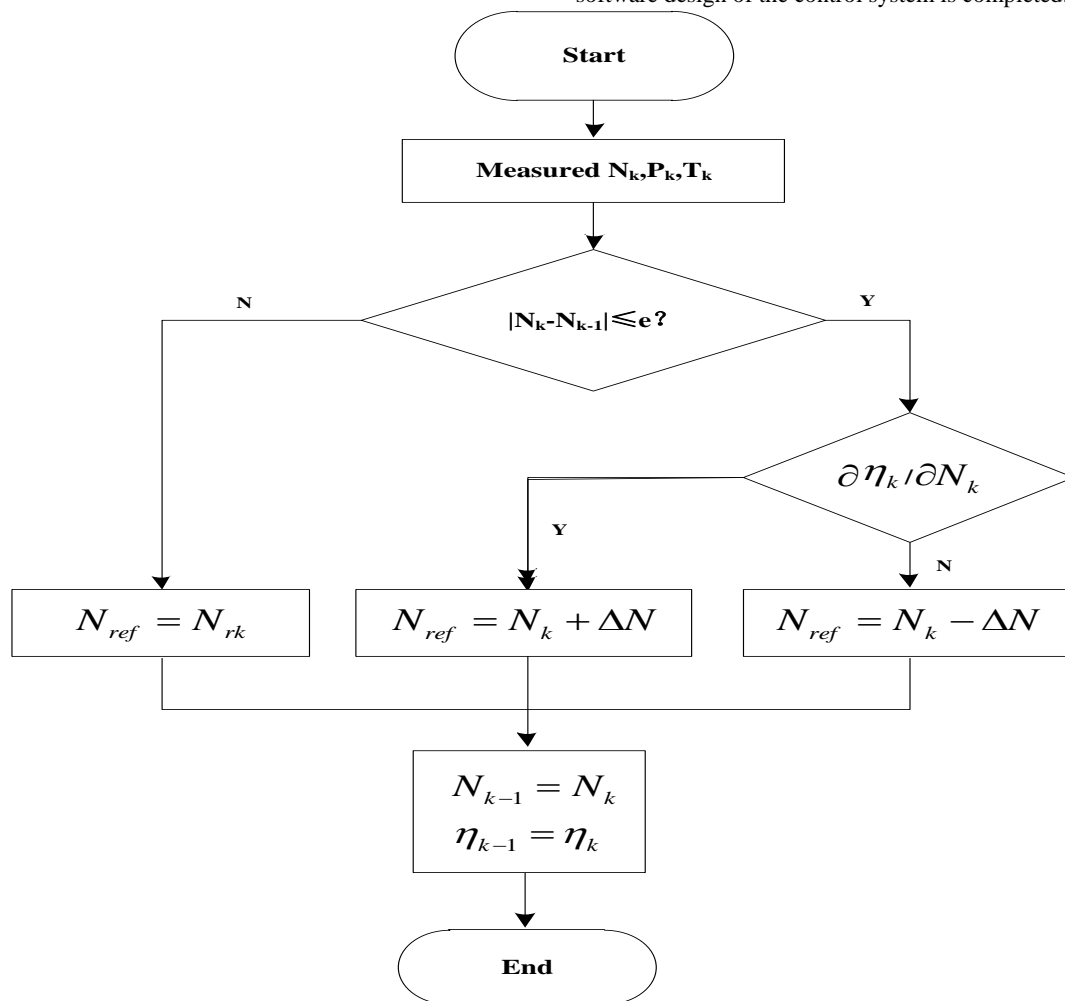


Figure 6. Maximum efficiency point tracking control process

4. Experimental results and analysis

In order to prove the application performance of the designed mechanical and electrical control system based on the tracking of maximum power point in the actual power work, the combined automatic generation control system of thermal power unit and energy storage system [2] in literature and the multi-port power generation control system based on energy storage [3] are set up as the experimental comparison system. In the same working environment, the mixed liquid gas is treated by three systems compressed energy storage is controlled by mechanical and electrical equipment.

4.1. Experimental platform and parameter setting

Based on the MATLAB/Simulink, the compression process of the system is taken as an example to simulate different control systems. Set up the experimental platform, as shown in Figure 7.

On the experimental platform shown in Figure 7, the inverter unit is controlled by the upper computer in the mixed liquid gas compressor and the permanent magnet synchronous motor is driven to drive the liquid pump to work, and the air is compressed to the air tank to realize energy conversion and storage. Figure 8 shows the mixed liquid gas compressor and accumulator.

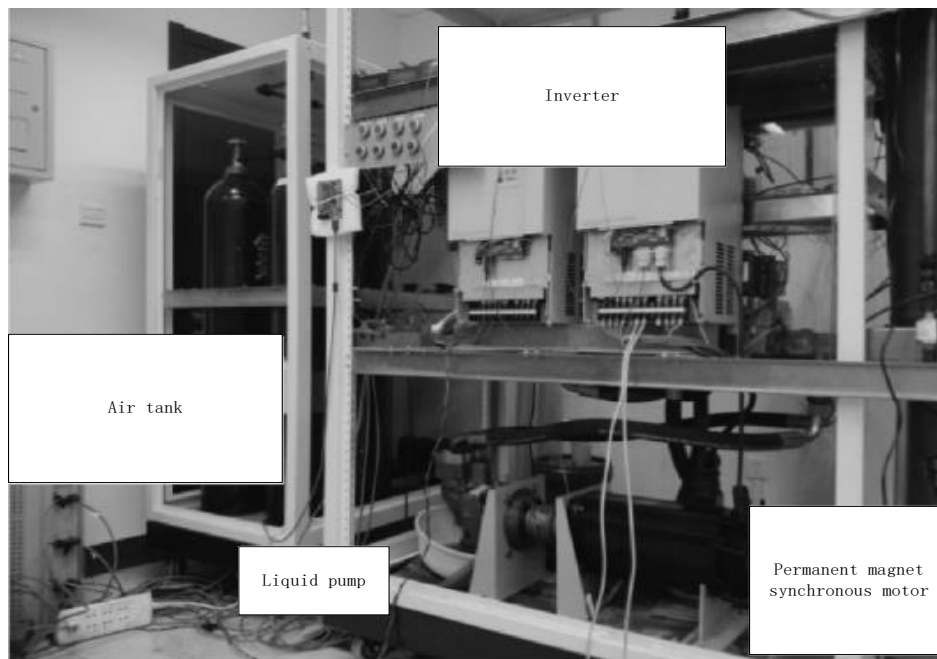


Figure 7. Experimental platform

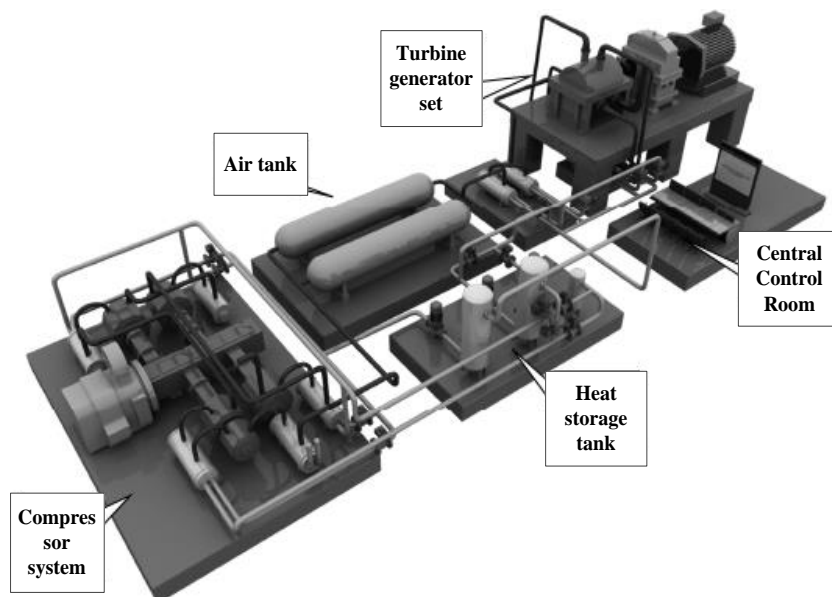


Figure 8. Mixed liquid gas compressor

Figure 8 comes from <http://www.njeiri.com/front/article/506.htm>. Through the experimental platform, the main parameters of the mixed liquid gas compressor and energy storage machine are set: the power is 15 kW; the rated power of the motor is 11 kW, the rated speed is 2000 r / min; the model of the liquid pump is Parker f12-125; the capacity of the air storage tank is 500 L; the maximum air storage pressure is 150bar (1bar = 1×10^5 Pa); the winding resistance (line line) of the motor is 0.3 Ω ; the winding inductance (line line) is 6.54 mh; the rotational inertia of the motor is 162.6 kg-cm². According to the above experimental platform and experimental parameter settings, two traditional control systems and the control system designed in this paper are used to carry out experiments, and the performance of the three control systems is compared.

4.2. Liquid pump efficiency

Based on the above experimental preparation, the efficiency of the liquid pump can be observed in real time in the upper computer interface by using the sensor signal and the upper computer using the above formula (6). The experimental waveform is shown in Figure 9.

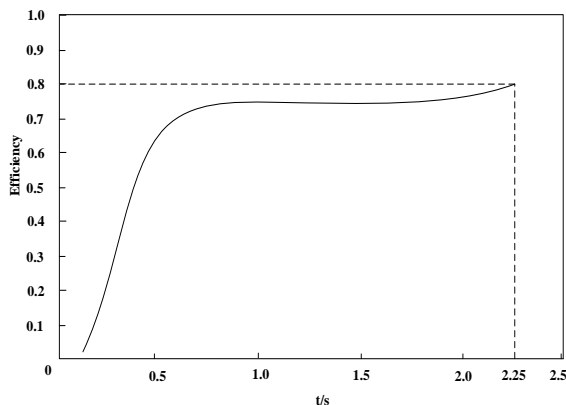


Figure 9. Efficiency of liquid pump

The input electric energy is measured by the electric energy meter at the interface between the experimental platform and the external power grid, and the following formula is used:

$$E = p_f V \ln\left(\frac{p_f}{p_0}\right) - p_0 V \left(\frac{p_f}{p_0} - 1\right) \quad (20)$$

In the above formula, p_f is the final gas pressure, p_0 is the initial gas pressure, and V is the gas volume. The results show that the efficiency of liquid pump is 0.52. Taking the efficiency of the liquid pump as the experimental index, the mechanical and electrical control system based on the tracking of the maximum power point, the automatic generation control system based on the combination of the thermal power unit and the energy storage system and the multi-port power generation control system based on the energy storage are compared and analyzed. The experimental results of the three control systems are shown in Table 2.

Table 2. Experimental results of three control systems

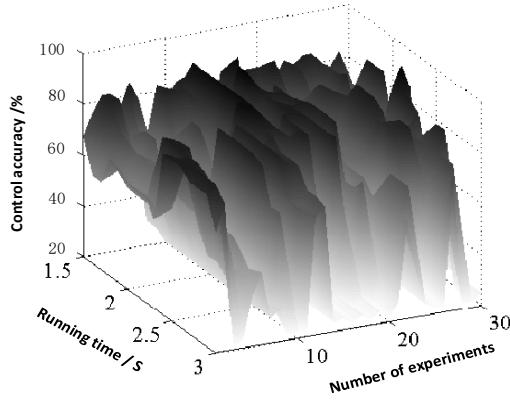
Control index of control system	Experimental result			
	Combined automatic generation control system of thermal power unit and energy storage system	Multi-port power generation control system based on energy storage	Mechanical and electrical control system of mixed liquid compressed energy storage based on maximum power point tracking	Contrast value
Input electric energy / (kW / h)	10.16	12.38	15.86	16.02
Storage energy / (kW / h)	5.42	7.31	8.30	8.33
Liquid pump efficiency	0.32	0.42	0.50	0.52

From the data shown in Table 2, it can be seen that under the same experimental platform, when the mechanical and electrical control system based on maximum power point tracking designed in this paper is used to control the mixed gas compressor, the efficiency of the system's liquid pump is the highest, and the system's liquid pump efficiency is the highest when the combined automatic generation control system of thermal power unit and energy storage system is used to control the mixed gas compressor. The efficiency of the system is slightly lower than that of the combined automatic generation control system of thermal power unit and energy storage system. Considering the waveform analysis of other parameters of the above system, the control system designed in this paper has high efficiency. However, there are some security risks in the joint automatic generation control system of thermal power unit and energy storage system and the multi-port power generation control system based on energy storage. Therefore, the mechanical and electrical control system based on maximum power point tracking designed in this paper is more efficient Suitable for energy storage system. Due to the loss of gas and liquid flow in the experiment, the experimental results of the mechanical and electrical control system based on maximum power point tracking are slightly lower than the given comparison value. Through simulation and experimental verification, it can be clearly seen that the control system designed in this paper improves the shortcomings of traditional control system based on the algorithm of maximum power point or maximum efficiency point.

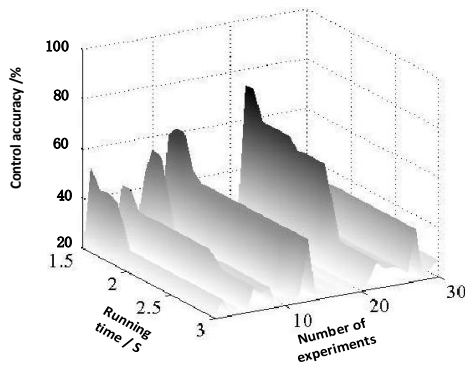
4.3. Control accuracy

In order to verify the effectiveness of the system in this paper, the mechanical and electrical control accuracy of the hybrid liquid gas compression energy storage system based on maximum power point tracking, the joint automatic power generation control system of thermal power unit and

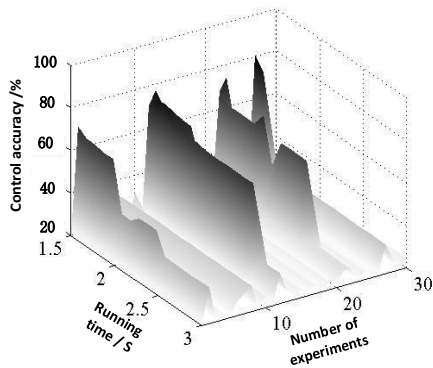
energy storage system and the hybrid liquid gas compression energy storage mechanical and electrical control accuracy of the multi-port power generation control system based on energy storage are compared and analyzed, and the comparison results are shown in Figure 10. The control accuracy = the working power of the system × 100% under ideal conditions.



(a) The control accuracy of this system



(b) Control accuracy of combined thermal power unit and energy storage system



(c) Control accuracy based on energy storage system

Figure 10. Comparison of control accuracy of different systems

According to Figure 10, the mechanical and electrical control accuracy of the designed mechanical and electrical control system based on maximum power point tracking is up to 90%, while the mechanical and electrical control accuracy of the combined automatic generation control system of thermal power unit and energy storage system and the multi-port power generation control system based on energy storage is up to 75% and 80%, which shows that the control accuracy of the system is higher than that of the traditional control system.

4.4. Active power

In order to further verify the effectiveness of the system designed in this paper, the mechanical and electrical control system based on maximum power point tracking, the combined automatic power generation control system of thermal power unit and energy storage system and the active power of the mixed liquid compressed energy storage system based on the multi-port power generation control system of energy storage are compared and analyzed. The comparison results are shown in Figure 11.

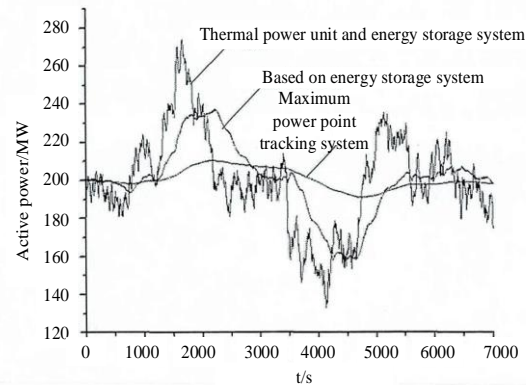


Figure 11. Comparison of active power of mixed liquid compressed energy storage

According to Figure 11, with the increase of operation time, the active power of the mechanical and electrical control system based on maximum power point tracking is between 190 MW and 210 MW, with a small change range; the active power of the system is between 130 MW and 280 MW; the active power of the hybrid liquid gas pressure storage system of the multi-port power generation control system based on energy storage is between 160 MW and 240 MW. The active power of the hybrid liquid gas pressure storage system of the combined automatic power generation control system of the thermal power unit and the energy storage system and the multi port power generation control system based on energy storage changes greatly. This shows that the active power of the hybrid liquid gas pressure storage system designed in this paper. The power is more stable than that of the traditional system.

5. Conclusion

With the development of energy storage system, the technological innovation of various energy storage methods is also in-depth. Compressed air energy storage technology as a relatively new way of energy storage, due to its unique advantages, has been widely concerned and actively studied by scholars all over the world. In this paper, a new type of compressed air energy storage system is designed. In the cycle of the compressed air energy storage system with liquid gas circulation, according to the different pressure range, the segmented compression ratio is determined, and the influence of this control mode on the efficiency is further analyzed. This refinement can keep the system in a quasi-constant temperature process and improve the efficiency of the system. The maximum efficiency point tracking control strategy of the hydraulic system is optimized. By setting the effective range of maximum efficiency point, the real-time performance of speed control is reduced. In the future, we need to complete the experiment on the experimental platform to solve the

problems in the experiment. The correctness of the simulation analysis and the feasibility of the system are verified by experiments.

Acknowledgement

The research is supported by: Tianjin Education Commission Scientific Research Program (Program NO. 2020KJ083).

References

- [1] Voznenko TI, Chepin EV, Urvanov GA. The control system based on extended BCI for a robotic wheelchair. *Procedia Computer Science*, 2018, 123:522-527.
- [2] Mu CH, Wu PY, Sun GH, et al. Frequency modulation technology and application of automatic generation control combined with thermal power unit and energy storage system. *Thermal Power Generation*, 2018, 47, 378(05):35-40.
- [3] Feng XT, Tao YY, Sun TT. Energy management and control strategy of multi port power system based on energy storage. *Electrical automation*, 2018, 40, 238(04):70-73.
- [4] Wang Y, Yang X, Liang H, et al. A review of the self-adaptive traffic signal control system based on future traffic environment. *Journal of Advanced Transportation*, 2018, 2018(PT.3):1096123.1-1096123.12.
- [5] Cuenca N, Antunes DJ, Castillo A, et al. Periodic event-triggered sampling and dual-rate control for a wireless networked control system with applications to UAVs. *Industrial Electronics, IEEE Transactions on*, 2019, 66(4):3157-3166.
- [6] Jeong SY, Park JH, Hong GP, et al. Autotuning control system by variation of self-inductance for dynamic wireless EV charging with small air gap. *IEEE Transactions on Power Electronics*, 2019, 34(6):5165-5174.
- [7] Kobayashi H, Kawagoe N, Kondo K, et al. Method to design control system of traction inverter of DC-electrified railway vehicle for an increase in regenerative brake power. *IEEJ Transactions on Industry Applications*, 2019, 139(1):30-39.
- [8] Gil JD, Roca L, Zaragoza G, et al. A feedback control system with reference governor for a solar membrane distillation pilot facility. *Renewable energy*, 2018, 120(MAY):536-549.
- [9] Xiao MZ, Pan W, Fei L, et al. Segmented power distribution control system based on hybrid cascaded multilevel converter with parts of energy storage. *IET Power Electronics*, 2018, 10(15):2076-2084.
- [10] Chang Z, Hu JK, Tao SR, et al. Simulation research on pressure stability optimization control of hydraulic cylinder of scraper. *Computer Simulation*, 2018, 35(06):248-251+466.
- [11] Antonolopoulos F, Petrakis EGM, Sotiriadis S, et al. A physical access control system on the cloud. *Procedia Computer Science*, 2018, 130:318-325.
- [12] Yue G, Pan YT, Zhang HJ, et al. A multi-neuron neural network algorithm for DSP servo control system of unmanned reconnaissance vehicle. *Beijing Ligong Daxue Xuebao/Transaction of Beijing Institute of Technology*, 2019, 39(2):203-208.
- [13] Venkatachalam V, Prabhakaran D, Thirumarimurugan M, et al. LMI based stability analysis of non-linearly perturbed DC motor speed control system with constant and time-varying delays. *International Journal of Power Electronics*, 2019, 10(1-2):1-17.
- [14] Wang WW, Liang X, Zhang MZ, et al. A new method for voidage correlation of gas-liquid mixture based on differential pressure fluctuation. *Chemical Engineering Science*, 2019, 193:15-26.
- [15] Xu H, Fan Y, Tong X, et al. Designing control system of hypersonic vehicle with dynamic pressure constraints considered. *Xibeigongye Daxue Xuebao/Journal of Northwestern Polytechnical University*, 2019, 37(1):41-47.